Published OnlineFirst August 18, 2020; DOI: 10.1158/1078-0432.CCR-20-1247

Tebentafusp, A TCR/Anti-CD3 Bispecific Fusion Protein Targeting gp100, Potently Activated Antitumor Immune Responses in Patients with Metastatic Melanoma

Mark R. Middleton[1], Cheryl McAlpine[2], Victoria K. Woodcock[1], Pippa Corrie[3], Jeffrey R. Infante[4], Neil M. Steven[5], Thomas R Jeffry Evans[6], Alan Anthoney[7], Alexander N. Shoushtari[8], Omid Hamid[9], Avinash Gupta[1], Antonella Vardeu[2], Emma Leach[2], Revashnee Naidoo[2], Sarah Stanhope[2], Sion Lewis[2], Jacob Hurst[2], Ita O'Kelly[2], and Mario Sznol[10]

ABSTRACT

Purpose: Tebentafusp is a first-in-class bispecific fusion protein designed to target gp100 (a melanoma-associated antigen) through a high affinity T-cell receptor (TCR) binding domain and an anti-CD3 T-cell engaging domain, which redirects T cells to kill gp100-expressing tumor cells. Here, we report a multicenter phase I/II trial of tebentafusp in metastatic melanoma (NCT01211262) focusing on the mechanism of action of tebentafusp.

Patients and Methods: Eighty-four patients with advanced melanoma received tebentafusp. Treatment efficacy, treatment-related adverse events, and biomarker assessments were performed for blood-derived and tumor biopsy samples obtained at baseline and on-treatment.

Results: Tebentafusp was generally well-tolerated and active in both patients with metastatic uveal melanoma and patients with metastatic cutaneous melanoma. A 1-year overall survival rate of 65% was achieved for both patient cohorts. On-treatment cytokine measurements were consistent with the induction of IFNγ pathway–related markers in the periphery and tumor. Notably, tebentafusp induced an increase in serum CXCL10 (a T-cell attractant) and a reduction in circulating $CXCR3^+$ $CD8^+$ T cells together with an increase in cytotoxic T cells in the tumor microenvironment. Furthermore, increased serum CXCL10 or the appearance of rash (likely due to cytotoxic T cells targeting gp100-expressing skin melanocytes) showed a positive association with patient survival.

Conclusions: These data suggest that redirecting T cells using a gp100-targeting TCR/anti-CD3 bispecific fusion protein may provide benefit to patients with metastatic melanoma. Furthermore, the activity observed in these two molecularly disparate melanoma classes hints at the broad therapeutic potential of tebentafusp.

Introduction

Reactivating the immune system with checkpoint inhibitors (CPIs) to treat cancer has seen significant success in the last decade (1) and is established as one of the pillars of cancer treatment (2). However, many patients derive little benefit from CPIs principally because of the lack of sufficient tumor-specific cytotoxic $CD8^+$ T cells or insufficient tumor neoantigenicity (3). Thus, new approaches that redirect any cytotoxic T cell to attack cancer cells may be key to achieving broader efficacy. Less than 10 years after the approval of the first CPI, the immuno-oncology field is now replete with novel approaches to engage the immune system to fight cancer (4, 5).

Natural T-cell responses are driven by interactions between the T-cell receptor (TCR) and its peptide antigen presented by HLA on the surface of a target cell (6). However, the TCR repertoire is limited by the thymic selection of T cells that recognize self-antigens with low affinity. To redirect any T cell, regardless of its TCR specificity, antibody- and TCR-based bispecifics that can activate T cells are being developed. Antibody-based bispecifics have demonstrated efficacy in hematologic tumors; however, the repertoire of antibody targets is limited to surface-expressed proteins and, thus, limited to targeting only 10% of the human proteome (7). In addition, antibody-based therapeutics only target highly expressed proteins. Immune-mobilizing monoclonal TCRs against cancer (ImmTAC) are a new class of molecules designed to overcome these limitations. These bispecific fusion proteins, comprising of a soluble affinity-enhanced TCR and an anti-CD3 single-chain variable fragment (scFv), redirect and activate T cells to peptide-HLA (pHLA) complexes on the target cell surface (4). As the majority of proteins are processed and presented on the surface of the cell as a pHLA complex, ImmTAC molecules could in principle be engineered to target almost the entire proteome (7). Tebentafusp, the first ImmTAC molecule to enter clinical testing, recognizes the gp100 peptide (pos 280–288) presented on HLA-A*02:01 with picomolar affinity. gp100 is a lineage melanocytic antigen expressed in melanocytes and melanoma. The high affinity of tebentafusp for the pHLA target seen in preclinical studies enables cells with low cell surface levels of HLA-A-$gp100_{280–288}$ to be detected: as few as five to 10 epitopes are sufficient for tebentafusp to mount successful clearance of target cells *in vitro* (8, 9). The anti-CD3 scFv effector domain of tebentafusp enables polyclonal activation of native

[1]Department of Oncology, Medical Sciences Division, University of Oxford, Headington, Oxford, United Kingdom. [2]Immunocore Ltd, Abingdon, Oxford, United Kingdom. [3]Cambridge University Hospitals, NHS Foundation Trust, Cambridge, United Kingdom. [4]Janssen, Philadelphia, Pennsylvania. [5]Institute of Immunology and Immunotherapy, College of Medical and Dental Sciences, University of Birmingham, Birmingham, United Kingdom. [6]Institute of Cancer Sciences, University of Glasgow, Glasgow, Scotland, United Kingdom. [7]Leeds Teaching Hospitals NHS Trust, Leeds, United Kingdom. [8]Memorial Sloan Kettering Cancer Center, New York, New York. [9]Immunooncology, The Angeles Clinic and Research Institute, Los Angeles, California. [10]Yale Cancer Center, Yale School of Medicine, Yale, Connecticut.

Note: Supplementary data for this article are available at Clinical Cancer Research Online (http://clincancerres.aacrjournals.org/).

Corresponding Author: Mark R. Middleton, University of Oxford, Old Road Campus Research Building, Headington, Oxford OX3 7LJ, United Kingdom. Phone: 4418-6561-7331; E-mail: mark.middleton@oncology.ox.ac.uk

Clin Cancer Res 2020;XX:XX–XX

doi: 10.1158/1078-0432.CCR-20-1247

Published OnlineFirst August 18, 2020; DOI: 10.1158/1078-0432.CCR-20-1247

Translational Relevance

The use of immunotherapeutic approaches for the treatment of metastatic disease has had some success in a subset of tumor types. However, limitations of success associated with tumor mutational burden are now recognized. Metastatic uveal melanoma (mUM) has low mutational burden and consequently, both lacks an immune response within the tumor and shows little response to checkpoint inhibitor therapies. Indeed, patients with mUM currently have few treatment options and have a poor prognosis with approximately 1 year median survival time after detection of metastases. Outcomes for these patients have not improved in decades and no new therapies have been approved for this subset of patients with melanoma for more than 30 years.

Here, we present data focusing on the mechanism of action of tebentafusp from a first-in-human study, in which patients with previously treated advanced metastatic melanoma (both cutaneous and uveal) received a soluble, affinity-enhanced T-cell receptor/anti-CD3 single-chain variable fragment fusion protein designed to facilitate targeting of T cells to the tumor. Our results suggest that tebentafusp is well-tolerated in both cancer cohorts and has clinically meaningful antitumor activity as a monotherapy. This is particularly impactful within the uveal melanoma cohort not only due to the absence of effective therapies, but also as it suggests this therapy can enhance immune responses in previously immune inactive tumors. These early data support further investigation of tebentafusp as a promising new anticancer therapy for metastatic melanoma.

T cells independently of their natural TCR specificity, leading to the formation of an immune synapse and the killing of target cells (refs. 8, 10; Supplementary Fig. S1). The *in vitro* capability of tebentafusp to induce potent and selective killing of antigen-positive tumor cells was demonstrated previously (9, 11). Furthermore, broad immune responses that extend beyond the induction of $CD8^+$ T-cell–mediated cytotoxicity were observed (8) and supported the progression of tebentafusp to phase I clinical investigations.

Patients and Methods

Study design and participants

This first-in-human (FIH) study of tebentafusp was a multicenter, phase I/II, open-label, dose-finding study to assess the safety, tolerability, and efficacy of tebentafusp (NCT01211262) in patients with stage IV or unresectable stage III melanoma, including cutaneous and uveal, who were resistant to standard treatment regimens or for whom no standard treatments existed. Additional key eligibility criteria included HLA-A*02 status, Eastern Cooperative Oncology Group performance status ≤1, as well as completed previous surgery, radiotherapy, systemic therapy, or experimental therapy.

The primary objectives of the trial were to evaluate the safety and tolerability of tebentafusp following weekly and daily dosing with the aim of establishing the MTD based on the occurrence of dose-limiting toxicity (DLT).

The study was performed in accordance with the current version of the Declaration of Helsinki, the International Conference on Harmonisation guidelines on Good Clinical Practice, and the laws of the United Kingdom and the United States. Institutional review board approval was gained on a site-by-site basis. All patients provided written informed consent to participate in the study prior to undergoing screening.

Eighty-four HLA-$A2^+$ patients with advanced melanoma [$n = 61$, cutaneous; $n = 19$, uveal; and $n = 4$, other origin (acral, lentiginous (vulval), mucosal (rectal), and unknown primary)] received tebentafusp (additional baseline demographics are presented in Supplementary Table S1).

Procedures

The study assessed a weekly (arm 1) and a daily (arm 2) dosing regimen for tebentafusp, each at a range of doses [arm 1 ($n = 66$): dose escalation, weight-based dosing from 5 to 900 ng/kg; dose expansion, 600 ng/kg converted to a 50-mcg flat dose and arm 2 ($n = 18$): once daily ×4 days every 3 weeks, dose ranges from 10 to 50 mcg; Supplementary Table S2].

Treatment efficacy was assessed using RECIST v1.1 and Kaplan–Meier survival. Treatment-related adverse events (TRAE) were coded according to Common Terminology Criteria for Adverse Events (CTCAE) v4.0. For "rash," any grade, composite terms included rash; rash erythematous; rash generalized and rash macular; rash maculopapular; rash papular; rash pruritic and rash pustular; and rash vesicular.

Biomarker assessments were performed for blood-derived and tumor biopsy samples obtained at baseline and on-treatment. Briefly, peripheral blood mononuclear cells (PBMCs) were stained for flow cytometric analysis and samples acquired with the BD Fortessa X20 HTS with BD FACSDiva v6. Compensation matrices and data analysis were performed with FlowLogic v7 software. The presence of cytokines/chemokines in serum samples was assessed using Luminex Bead-based Multiplexing Kits and acquired with xPONENT software version 4.2 SECURITY on a MAGPIX instrument. Multiplex gene expression analysis was carried out on RNA isolated from tumor biopsies using NanoString Technology. Tumor biopsy samples were sectioned and stained by single-plex IHC for CD3, CD4, CD8, granzyme B, or PD-L1 positivity. Images were acquired with either the Aperio (Leica Microsystems Ltd) or the Pannoramic MIDI (3DHISTECH) Whole-Slide Scanner and analyzed using HALO software. Additional details of the procedure are included in the Supplementary Materials and Methods.

For the four modes of analysis (serum markers, PBMC analysis, paired biopsies IHC, and gene analysis) described, six metastatic cutaneous melanoma (mCM) patient samples were analyzed by all four analyses. One metastatic uveal melanoma (mUM) patient sample was analyzed by all, but NanoString analysis, while two additional mCM samples were analyzed by serum markers, PBMC, and NanoString analysis, but not paired IHC. Twenty-two (11 mUM, 10 mCM, and one unknown primary) samples had serum and PBMC analysis.

Outcomes

Treatment efficacy was assessed using RECIST v1.1 and Kaplan–Meier survival. The efficacy population included patients with (i) at least one RECIST 1.1 evaluable target lesion, (ii) who were treated with (a) at least one tebentafusp dose of ≥270 ng/kg (a median absolute dose of ≥16 mcg) or (b) the recommended phase II dose (RP2D, 50 mcg), and (iii) who received at least one end-of-cycle scan or discontinued prior to the scheduled scan. Overall survival (OS) was measured from the start of treatment to time of death. Patients alive at the time of the analysis were censored on the last date they were known to be alive. TRAEs were coded according to CTCAE v4.0. To explore tebentafusp's effects on peripheral cytokine/chemokine profiles and T-cell number and phenotype, markers in serum and PBMC samples were analyzed in

Published OnlineFirst August 18, 2020; DOI: 10.1158/1078-0432.CCR-20-1247

baseline and on-treatment samples. T-cell infiltration and gene expression profile were assessed, comparing baseline and on-treatment tumor biopsy analysis.

Statistical analysis

Statistical analyses were performed as described in the figure legends. Survival analysis was carried out using Kaplan–Meier curves (R package, survminer) and log-rank test was used to assess differences between the survival curves. Univariate Cox proportional hazards methods were used to model the prognostic importance of potential predictors of survival. Fisher exact test was used to assess association of biomarker response with the maximum percentage reduction in the sum of longest diameters (SLDs) of tumor measurements from baseline. Spearman correlations were used to measure the association between different types of biomarker responses. Differences in percentage of a given phenotypic subpopulation, on-treatment relative to baseline, were calculated by Wilcoxon signed-rank test for paired data. NanoString tumor gene expression analysis comparing the $\log_2$ fold change between baseline and early postdose samples between patient groups using *t* tests was performed. The differential genes ($P < 0.05$) were then accessed for enrichment of 21 NanoString predefined categories, using hypergeometric tests (12). Those genes that fell into these significantly enriched categories were then presented in a heatmap displaying the pre/postdose $\log_2$ fold change values. Heatmaps were constructed using the ComplexHeatmap R library (13).

Results

Eighty-four HLA-A2$^+$ patients with advanced melanoma ($n = 61$, mCM; $n = 19$, mUM; and $n = 4$, other origin) were treated and evaluated: 31 patients with a weekly dose regimen of 5–900 ng/kg and 18 patients with daily dose regimen of 10–50 mcg (for 4 consecutive days every 3 weeks). Repeat dosing with tebentafusp continued as long as, in the opinion of the investigator, the patient was deriving clinical benefit and the benefit–risk ratio remained favorable. The median duration of treatment was 66 days, and eight of 84 patients were on-treatment for a year or longer. Thirty-five patients were treated with weekly doses of 600 ng/kg or 50 mcg with no patient experiencing DLT during the first 8 days after treatment. At the 900 ng/kg dose, two of four patients experienced DLT of hypotension, indicating that per protocol, the MTD had been exceeded. Three more patients were treated with the 600 ng/kg dose, and none reported a DLT. The MTD was identified as 600 ng/kg and RP2D for weekly dosing was set as 68 mcg. Eighty-three (99%) patients had ≥1 TRAEs of any grade (**Table 1**), while two patients (2.4%) experienced drug-related AEs leading to treatment discontinuation. The most common grade ≥3 TRAEs were rash (26% total, 20% arm 1, and 39% arm 2) and lymphopenia (13% total, 14% arm1, and 11% arm2), possibly mechanism-related, consistent with an on-target effect specific to melanocytic gp100 and peripheral T-cell redirection.

Cytokine release syndrome (CRS), which has been described with other T-cell–activating bispecifics, was evaluated *post hoc* (**Table 1**; ref. 14). The incidence of any grade CRS was 60%, the majority of which were generally mild with transient fever, fatigue, nausea, and headache; with no grade 3 or above CRS reported.

One-year OS rate of 65% (95% confidence interval, 48–78) was achieved, with similar survival recorded for both patients with mUM and patients with mCM (**Fig. 1**). Overall response rate by RECIST v1.1 (15) was 8.7% (six responses, all partial response; PR) with a further 38 patients (55%) categorized as stable disease, of which five patients (7.2%) showed minor responses (Supplementary Table S3). For the six patients who achieved a PR, three (16%) were from the mUM patient population. The median duration of response was 10.5 months (range, 3.7–28.2) and survival (censored at last contact) was 33.4 months (range, 13.9–47.2).

To examine the effect of tebentafusp on immune activation in patients with metastatic melanoma and to assess whether immune activation translates into antitumor activity, pre- and on-treatment serum samples and PBMCs, available from patient subsets, were used to determine cytokine/chemokine levels and the phenotype of circulating CD4$^+$ and CD8$^+$ T-cell subpopulations and correlated with clinical outcomes. The majority of patients with biomarker data were treated with a weekly dose of 600 ng/kg or 50 mcg.

Changes in serum markers in response to tebentafusp were determined through multiplex analyses. Thirty-two markers of immune modulation, IFNγ-dependent pathways, chemokines, as well as markers of angiogenesis, cell adhesion, and extracellular matrix (ECM) modulation were analyzed for up to 40 patients (13 mUM, 25 mCM, one lentiginous, and one unknown primary; **Fig. 2A**). In response to the first dose of tebentafusp, more than half of patients in the analyzed subset exhibited a treatment-induced increase of at least twofold from baseline for the following markers: CXCL10, CXCL11, CXCL9, CCL2, IFNγ, IL6, IL10, IL2, IL15, IL1RA, TNFα, GCSF, CCL27, HGF, and IL4, whereas other markers including IL17, IL5, IL1b, IL12p70, and GMCSF showed negligible detectable changes in most (≥90%) patients. The five markers with the greatest magnitude of treatment-induced increase included the IFN-inducible chemokines CXCL10 (median, 66-fold and range, 414-fold) and CXCL11 (median, sevenfold and range, 120-fold), as well as IL2, IL6, and IL10. Across all the serum markers analyzed, CXCL10 showed the greatest increase in the majority of patients analyzed in both mUM and mCM cohorts.

Temporal analysis showed the induction of serum cytokines to be transient, reaching maximal levels 8–24 hours postdose, with the profile returning toward baseline levels prior to the next dose, while notably, CXCL10 remained elevated relative to baseline levels (**Fig. 2B**). The induction of cytokines was attenuated after repeated weekly dosing, suggestive of a tachyphylactic immune response (**Fig. 2B**).

Given previous *in vitro* data demonstrating tebentafusp-induced redirection and activation of effector and memory cells from both CD8$^+$ and CD4$^+$ T-cell populations (8), and together with the observation here that, the most pronounced serum pharmacodynamics impact of tebentafusp was an increase in chemokine CXCL10, we hypothesized that tebentafusp treatment would preferentially redirect CD4$^+$ and CD8$^+$ T-cell subsets expressing the cognate receptor, CXCR3. This chemoattractant receptor has a key role in the trafficking of Th1 and CD8$^+$ T cells to peripheral sites of Th1-type inflammation and establishing the Th1 amplification loop mediated by IFNγ and the IFNγ-inducible CXCR3 ligands (16).

Immunophenotyping analysis was performed on PBMC samples from 22 patients (11 mUM, 10 mCM, and one unknown primary). Analysis of on-treatment PBMC samples showed that there was a relative reduction in the prevalence of CXCR3$^+$ immune cell populations that was more evident in CD8$^+$ versus CD4$^+$ populations (**Fig. 2C**); consistent with their higher baseline CXCR3 expression levels (Supplementary Fig. S2). On-treatment response of CXCR3$^+$ CD8$^+$ subsets was compared at 8, 24, and 48 hours after first dose. The largest relative decrease at 24 hours was observed for memory CD8$^+$ T-cell subsets, which was sustained at 48 hours (Supplementary Fig. S3).

Published OnlineFirst August 18, 2020; DOI: 10.1158/1078-0432.CCR-20-1247

Table 1. Most frequent TRAEs (shown for both any grade and grades ≥3) observed in FIH phase 1 study of tebentafusp split by study arm and also shown as total number.

TRAEs	Total ($N = 84$)					
	All grades, *n* (%)			Grade ≥3, *n* (%)		
	Arm 1	Arm 2	Total	Arm 1	Arm 2	Total
Any TRAE	65 (98)	18 (100)	83 (99)	27 (41)	9 (50)	36 (43)
CRS[a]			50 (60)[b]			0 (0)
Other CRS-related AE[c]			8 (10)			8 (10)
Rash[d]	47 (71)	10 (56)	57 (68)	13 (20)	7 (39)	22 (26)
Pruritus	43 (65)	16 (89)	59 (70)	0 (0)	1 (6)	1 (1)
Pyrexia	35 (53)	13 (72)	48 (57)	3 (4)	1 (6)	4 (5)
Periorbital edema	30 (45)	11 (61)	41 (49)	0 (0)	0 (0)	0 (0)
Fatigue	35 (53)	10 (56)	45 (54)	0 (0)	0 (0)	0 (0)
Nausea	34 (51)	10 (56)	44 (52)	0 (0)	0 (0)	0 (0)
Hypotension	21 (32)	7 (39)	28 (33)	6 (9)	1 (6)	7 (8)
Vomiting	24 (36)	10 (56)	34 (40)	0 (0)	0 (0)	0 (0)
Chills	17 (26)	9 (50)	26 (31)	0 (0)	0 (0)	0 (0)
Skin exfoliation	19 (29)	5 (28)	24 (29)	0 (0)	0 (0)	0 (0)
Dry skin	18 (27)	5 (28)	23 (27)	0 (0)	0 (0)	0 (0)
Headache	16 (24)	6 (33)	22 (26)	0 (0)	0 (0)	0 (0)
Erythema	17 (26)	2 (11)	19 (23)	0 (0)	0 (0)	0 (0)
Lymphopenia	13 (20)	4 (22)	17 (20)	9 (14)	2 (11)	11 (13)
Hypophosphatemia	5 (8)	3 (17)	8 (10)	3 (4)	2 (11)	5 (6)

[a]TRAEs (any grade) per investigator that were also cytokine-mediated per Lee criteria (14) were mostly mild to moderate.
[b]Both events occurred within the first 21 days. One of these patients had a second event of lower grade (grade 1) that occurred after day 21.
[c]AEs were potentially consistent with CRS (e.g., infusion-related reaction, severe drug reaction, systemic inflammatory response syndrome, and hypotension). No CRS-related deaths occurred. Premedication with corticosteroids was not required in the protocol.
[d]Rash, as described here, is a composite term including the preferred terms; rash; rash erythematous; rash generalized and rash macular; rash maculo-papular; rash papular; and rash pruritic and rash vesicular.

Linking the observed marked tebentafusp-induced pharmacodynamics changes in CXCL10 and CXCR3$^+$ CD8$^+$ T cells, we found a greater increase in serum CXCL10 was associated with a greater transient reduction in peripheral CXCR3$^+$ CD8$^+$ T cells at all three time points examined, with the strongest association at 24 hours after first treatment (**Fig. 2D**; $R = -0.66$; $P = 0.00104$). Within the CXCR3$^+$ CD8$^+$ T-cell pool, an increase in serum CXCL10 was associated with concomitant reduction in cells with an effector memory phenotype (EM; $P = 0.03$, 0.007, and 0.02, and late differentiated/effector memory re-expressing CD45RA; $P = 0.02$, 0.03, and 0.003) at 8, 24, and 48 hours (Supplementary Table S4). In contrast, for memory CD4$^+$ T cells, significant correlations with increased CXCL10 were only observed at the later time points of 24 ($P = 0.006$) and 48 hours ($P = 0.01$) for EM and 48 hours for central memory (CM, $P = 0.002$) and stem cell memory T cell (Tscm, $P = 0.004$). At 24 hours after first treatment, generally reflective of maximal temporal change, the reduction in peripheral CXCR3$^+$ CD8$^+$ EM cells also correlated with serum increase in the other IFNγ-inducible CXCR3 receptor ligands, CXCL11 ($P = 0.04$) and CXCL9 ($P = 0.008$; Supplementary Table S4). In contrast, no relationship was evident for other tebentafusp-induced serum markers that are known chemoattractants for B cells (CXCL13), eosinophils (CCL11), and neutrophils (CXCL8).

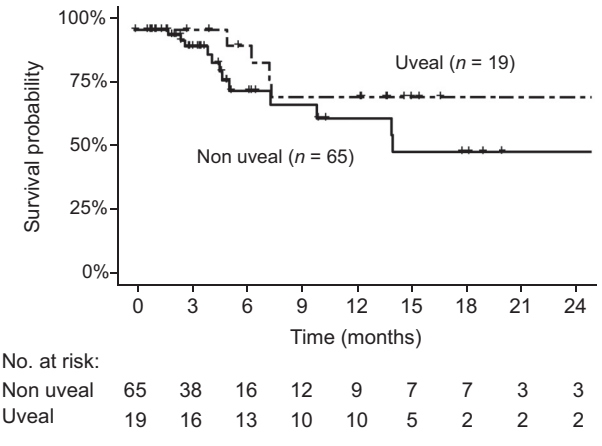

Figure 1.
One-year OS for tebentafusp-treated patients with mUV and mCM.

To assess changes in T cells in the tumor microenvironment following tebentafusp treatment, paired pre- and posttreatment tumor biopsy IHC analyses (melanoma type: one mUM, 7–8 mCM, one lentiginous, and one acral) revealed that most posttreatment biopsy samples (taken 3–17 days after first tebentafusp treatment) had a relatively greater presence of T-cell markers compared with pretreatment (**Fig. 3A**). At least a twofold increase in the number of intratumoral T cells was evident in most on-treatment biopsies relative to paired pretreatment samples: CD3$^+$ ($n = 8/11$ evaluable patients), and CD4$^+$ and CD8$^+$ ($n = 5/10$ evaluable patients). Furthermore, an increase in CD8$^+$ cells on-treatment was seen even in patients with relatively few intratumoral T cells prior to treatment, as exemplified by the patient with mUM in the IHC paired dataset (**Fig. 3B**, patient C). At least a twofold increase in PD-L1 expression was also observed in five of nine patients (**Fig. 3A**), and treatment with tebentafusp did not induce loss of gp100 expression, as evidenced by the median gp100 expression pre- and posttreatment (median 54.1%, $n = 16$ pre- vs. 52.9%, $n = 25$ posttreatment; Supplementary Fig. S4).

To more broadly assess the changes in the tumor immune microenvironment following tebentafusp, we analyzed gene expression from

Published OnlineFirst August 18, 2020; DOI: 10.1158/1078-0432.CCR-20-1247

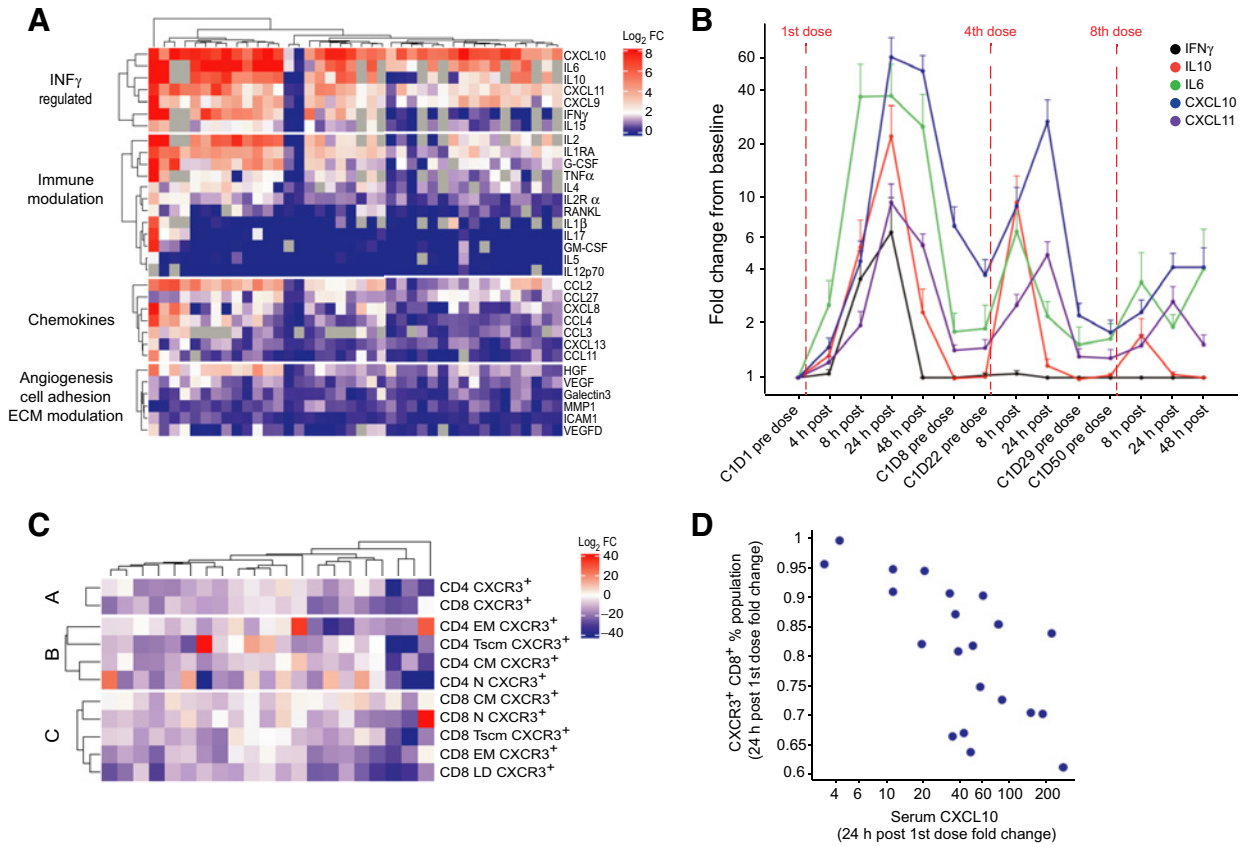

Figure 2.

Tebentafusp induced a pharmacodynamics response in multiple peripheral immune markers. **A,** Maximal postdose (log_2) fold-change, relative to baseline concentration, in response to first dose in serum markers in a subset of 40 patients: CXCL8, MMP-1, CXCL10, CCL2, VEGF, CXCL13, IL1RA, galectin 3, CCL3, CCL4, IL4, IL17, GM-CSF, IL2Rα, RANKL, CXCL9, IL5, G-CSF, IL12p70, ICAM-1, CXCL11, HGF, VEGFD, CCL27, and CCL11 ($n = 40$); and IFNγ, TNFα, IL1β, IL2, IL6, IL10, and IL15 ($n = 31/40$; ECM). **B,** Temporal profile of after first, fourth, and eight dose fold-change response in IFNγ, IL10, IL6, CXCL10, and CXCL11 in a subset of 15 patients treated weekly with 600 ng/kg or 50-mcg tebentafusp. Plots represents mean ± SEM. **C,** Percentage differences in $CXCR3^+$ $CD4^+$ and $CD8^+$ parent populations (A), $CD4^+$ subsets (B), and $CD8^+$ subsets (C) at approximately 24 hours after first dose of tebentafusp compared with baseline. Heatmaps constructed using the ComplexHeatmap R library (13). N, naïve and LD, late differentiated EM. **D,** Correlation of fold increase in serum CXCL10 with fold decrease in peripheral $CXCR3^+$ $CD8^+$ cell population 24 hours following first dose of tebentafusp ($R = -0.66$; $P = 0.00104$; $n = 21$).

paired baseline and on-treatment biopsies. We compared the gene expression within a subset of nine patients (melanoma type: one mUM, six mCM, one lentiginous, and one acral): two responders (PR) and seven with progressive disease. Enrichment analysis of significantly different genes comparing on-treatment changes in tumor biopsies from PR compared with progressive disease patients found three categories of genes, defined *a priori*, to be significantly enriched: cytotoxicity (7/10 genes, $P = 0.00007$), antigen processing (8/22, $P = 0.006$), and T-cell functions (16/72, $P = 0.029$; **Fig. 3C**).

In the study of mechanism of action for any therapy, biomarker analysis provides important insight, and the association of biomarkers with positive clinical outcome adds tangible value from a clinical perspective. The relative relationships between measured peripheral biomarkers and clinical outcomes were examined.

Maximal transient increase in serum CXCL10 level was typically noted in response to the first dose of tebentafusp (**Fig. 2B**). Within this subset of patients, data suggest that a greater maximal fold increase was associated with both longer OS (**Fig. 4A**; $P = 0.00019$) and greater tumor shrinkage (**Fig. 4B**; $P = 0.0029$). Higher treatment-induced levels of CXCL11, another CXCR3 ligand, were also associated with longer OS (Supplementary Fig. S5). For the transient reduction in circulating $CXCR3^+$ $CD8^+$ T-cell population in response to first dose of tebentafusp, a greater decrease was associated with longer OS (**Fig. 4C**; $P = 0.0086$) and greater tumor shrinkage (**Fig. 4D**; $P = 0.03$).

The majority of patients treated with tebentafusp developed rash within the first few days of dosing, consistent with cytotoxic T cells being redirected to attack gp100-expressing melanocytes in the skin. Of the 84 patients treated, 69 (82%) experienced any "rash" (refer to Patients and Methods for composite terms; **Table 1**) of any grade occurring within 21 days of first dose; these patients survived longer than those who did not have rash ($P = 0.003$, **Fig. 5A**; Supplementary Table S5) and this was independent of absolute lymphocyte count and prior anti–PD-1 therapy in a multivariate analysis. Patients with "rash" had a relatively greater maximal on-treatment peripheral response: increase in serum CXCL10 level and decrease in $CXCR3^+$ $CD8^+$ T-cell population (**Fig. 5B** and **C**).

Discussion

Tumors escape the immune system through the cooperative processes of central and peripheral tolerance. Overcoming peripheral tolerance through CPI or administration of cytokines has delivered long-term patient benefit in the treatment of some neoplasms (1), and

Published OnlineFirst August 18, 2020; DOI: 10.1158/1078-0432.CCR-20-1247

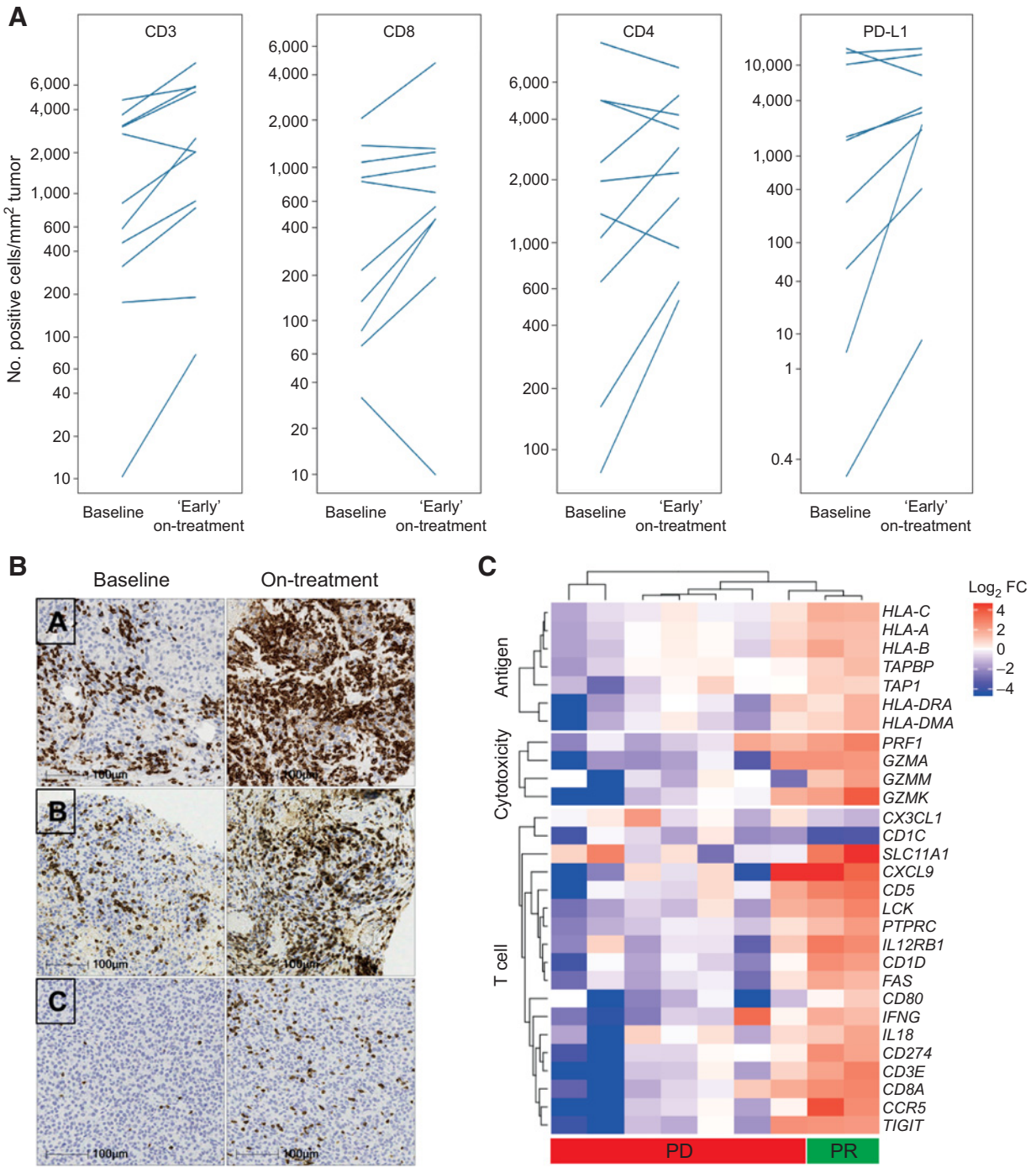

Figure 3.

Increased presence of T cells observed in on-treatment tumors. Image analysis quantified the expression of $CD3^+$, $CD4^+$, or $CD8^+$ T cells together with PD-L1 expression. **A,** Number of $CD3^+$, $CD8^+$, $CD4^+$, and PD-$L1^+$ cells/mm^2 tumor in paired baseline and early on-treatment biopsies (taken at cycle 1 day 3–17) from up to 11 patients; line per patient. **B,** Representative IHC images of $CD3^+$ staining in baseline and on-treatment (C1D3) biopsies from three patients: nonuveal patient A (rectus abdominal muscle) and B (L abdomen); uveal patient C (abdominal wall). **C,** Heatmap representation of genes identified from enrichment analysis with significantly different expression in on-treatment tumor biopsy (taken at cycle 1 day 3–17) relative to baseline sample from PR compared with progressive disease patients. These genes belonged to NanoString categories "antigen processing," "cytotoxicity," or "T-cell function" (*HLA-C, -A, -B* also in antigen processing and cytotoxicity category). Data scale represents log_2 fold-change relative to associated baseline.

Published OnlineFirst August 18, 2020; DOI: 10.1158/1078-0432.CCR-20-1247

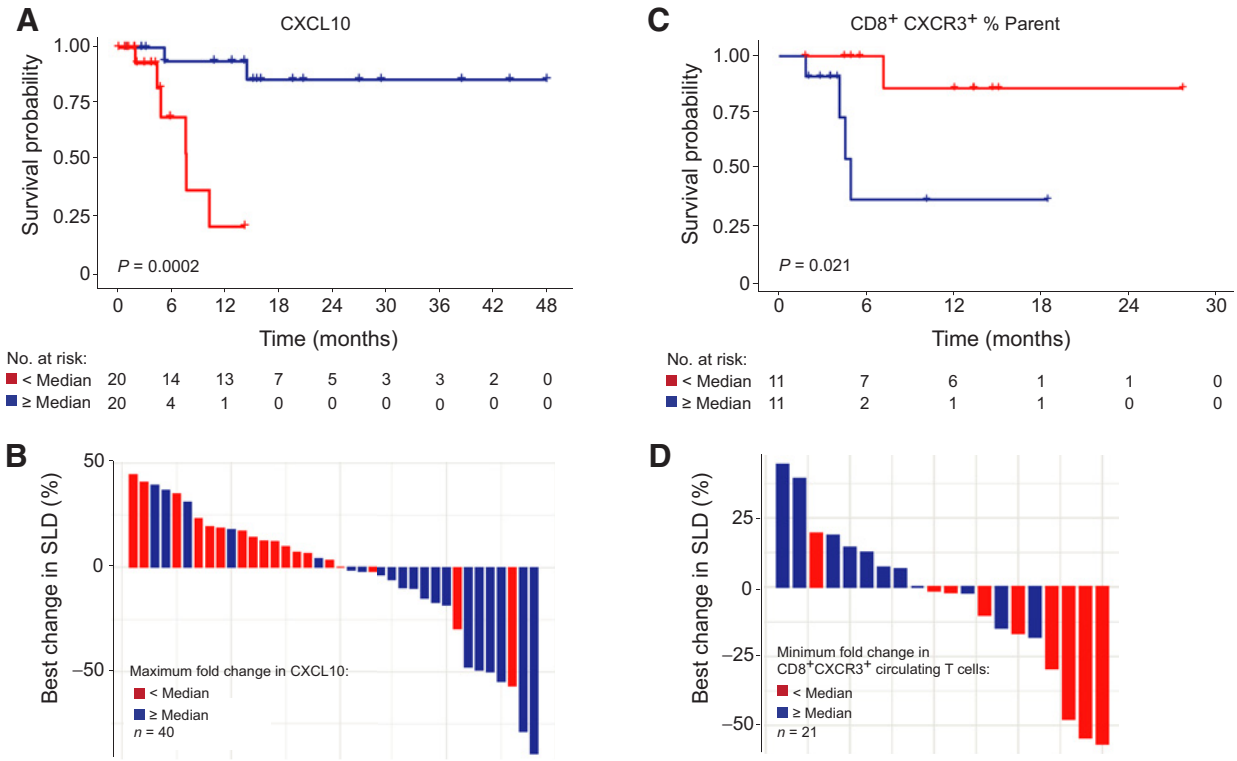

Figure 4.

On-treatment biomarkers associated with clinical response. A greater maximal fold increase in serum CXCL10 level, and maximal fold decrease in circulating CXCR3$^+$ CD8$^+$ T-cell population in response to first dose of tebentafusp, was associated with longer OS and tumor shrinkage. Kaplan–Meier survival of patients by: serum CXCL10 ($n = 40$, $P = 0.00019$; **A**) and CXCR3$^+$ CD8$^+$ T-cell population ($n = 22$, $P = 0.0086$; **C**); both ≥median versus <median. Waterfall plots depicting the maximum percentage reduction in the SLDs of target tumor measurements from baseline for change in serum CXCL10 (Fisher exact test, $P = 0.0029$; **B**) and CXCR3$^+$ CD8$^+$ T cells (Fisher exact test, $P = 0.03$; **D**), both ≥median versus <median.

these agents are changing the landscape of cancer therapy. However, accumulating evidence suggests that efficacy of agents focused on breaking peripheral tolerance may be limited to inflamed tumors (those with tumor-infiltrating immune cells) and that patients with immune-deserted (or immunologically ignorant) tumors fail to have long-term benefit due to inadequate tumor-specific CD8$^+$ T cells or insufficient neoantigenicity (17).

Tebentafusp is the first soluble TCR bispecific (ImmTAC molecule) to demonstrate antitumor activity by bypassing central tolerance and redirecting polyclonal T cells to kill tumor cells expressing target antigens (4, 9). Data presented here demonstrate tebentafusp monotherapy was well-tolerated and active in patients with mUM and mCM. The on-treatment response profile was consistent with the induction of IFNγ pathway–related markers in the periphery and tumor. On-treatment increase in T cells within the tumor microenvironment, together with concomitant increase in peripheral IFNγ-inducible chemokines (CXCL9, CXCL10, and CXCL11) and reduced circulating CXCR3$^+$ T cells, provide strong evidence for the mechanistic role of this chemoattractant axis in T-cell redirection by tebentafusp.

The importance of CXCL10 recruitment of tumor-suppressive CXCR3$^+$ T cells has been demonstrated in other solid cancer models (18, 19) and high intratumoral concentration was associated with a higher lymphocytic infiltrate (18) and an improved survival in several malignancies, including metastatic melanoma (20–23). Similarly, data from HER2–CD3 bispecific preclinical murine studies have previously suggested a mechanistic role for CXCL10–CXCR3 axis in tumor response (24). A role of this axis in the sensitivity to anti–PD-1 therapy has also been indicated (25). In contrast to the relative lack of peripheral biomarkers of response identified for CPI treatments, data presented here suggest potential dynamic markers for tebentafusp.

Adverse effects from tebentafusp were consistent with its observed *in vitro* mechanism of action (4, 11, 26). For example, rash and pruritus (likely due to targeting of T cells to gp100$^+$ melanocytes) or cytokine-mediated AEs, such as fever, are expected for a bispecific molecule such as tebentafusp. The temporal association between some of these AEs and key peripheral cytokines underscores the apparent mechanistic relationship. Furthermore, the occurrence of rash appeared to be associated with longer survival and related to a greater peripheral CXCL10 and CXCR3$^+$ T-cell response.

In the limited number of on-treatment tumor biopsies that were available, tebentafusp treatment was associated with increased numbers of CD4$^+$ and CD8$^+$ T cells. While numbers were small and evaluation was across both arms and tumor types, genes associated with T-cell function, antigen processing, and cytotoxicity were significantly greater in biopsies from partial responders compared with those with progressive disease. This response was evident even in patients with low levels of tumor-infiltrating lymphocytes prior to treatment, including uveal melanoma, suggesting that tebentafusp may be useful broadly in the treatment of patients regardless of baseline tumor-infiltrating lymphocytes.

The antitumor activity observed for tebentafusp monotherapy (reduction in target tumor SLD and extended survival) in patients

Published OnlineFirst August 18, 2020; DOI: 10.1158/1078-0432.CCR-20-1247

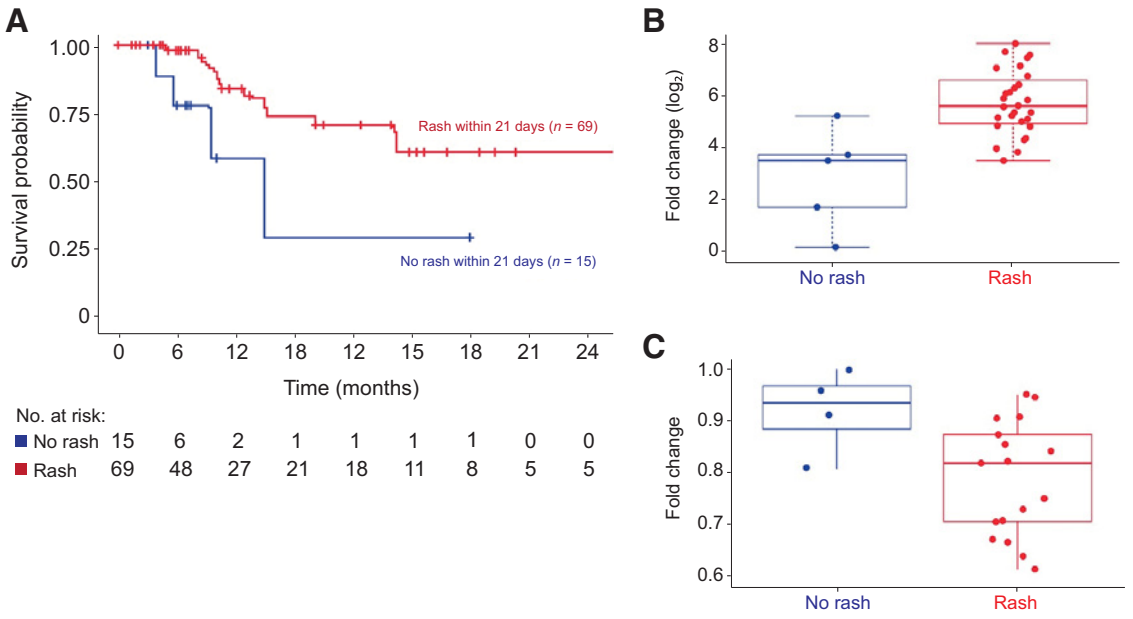

Figure 5.

Rash associated with patient survival and elevated serum CXCR10. **A,** Kaplan–Meier survival of patients with any "rash" (refer to Patients and Methods) within 21 days of treatment start ($n = 69$) versus no rash reported ($n = 15$; $P = 0.028$). Patients with "rash" had tendency for greater on-treatment maximal fold-change in serum CXCL10 ("rash" $n = 34$ vs. no rash $n = 6$, $P = 0.001$; **B**) and circulating CXCR3$^+$ CD8$^+$ T cells ("rash" $n = 17$ vs. no rash $n = 4$, $P = 0.04$; **C**). Box plot representation of fold-change relative to baseline, showing median and quartiles for each group.

with mUM within this trial is promising for this rare cancer with high unmet medical need (26). Uveal melanoma arises from melanocytes within the uveal tract of the eye (27, 28) and metastasizes in half of patients, with 90% of these patients developing metastases to the liver (17, 29). mUM has a poor prognosis with 1-year survival rate of 10%–40% from development of metastases (30). The limitations in the treatment options for mUM, with no universally recognized standardized treatment and no new medicines approved for this subset of patients with melanoma in the past 30 years, are reflected in the failure to improve OS in the last 50 years (31).

Importantly, in contrast to mCM, mUM has a low tumor mutational burden and is relatively insensitive to CPI (32). Therefore, the antitumor activity observed within this trial with two molecularly diverse tumor types, suggests the possibility of the broad therapeutic potential of tebentafusp in tumors with a high mutational burden and sensitive to CPI (CM) and in those with a low mutational burden, immunologically barren, and insensitive to CPI (UM). Trials of tebentafusp in patients with uveal melanoma are underway to confirm and extend these findings.

Disclosure of Potential Conflicts of Interest

M.R. Middleton reports personal fees and other from Immunocore (trial fees) during the conduct of the study and other from BMS (trial fees), Merck/MSD (trial fees), Regeneron (trial fees), and Replimune (trial fees) outside the submitted work. C. McAlpine reports other from Immunocore (employment) during the conduct of the study. V.K. Woodcock reports other from Immunocore (trial fees) during the conduct of the study, BMS (trial fees), MSD (trial fees), Regeneron (trial fees), and Replimune (trial fees) outside the submitted work. P. Corrie reports other from Cambridge University Hospitals NHS Foundation Trust (reimbursement of research activities associated with patients recruited in this clinical trial, paid to institution) during the conduct of the study and Cambridge University Hospitals NHS Foundation Trust (payment to conduct other commercial-sponsored clinical trials associated with evaluating melanoma therapeutics) outside the submitted work. J.R. Infante reports personal fees from Janssen Oncology (employment) during the conduct of the study and outside the submitted work. N.M. Steven reports personal fees from University of Birmingham (in around 2011 received a fee for supporting Immunocore to present data to the regulatory bodies) and Merck Serono (teaching provided for fee paid directly to employer) and Incyte (advisory board 2017) outside the submitted work and other from University of Birmingham (institution was paid on a per item basis for patient recruitment and deliver of the clinical trial) during the conduct of the study. T.R.J. Evans reports grants and other from Immunocore (support for costs of clinical trials payable to the institution) during the conduct of the study, grants, personal fees, and other from MSD (support for costs of clinical trials, honoraria for speaker's fees and consultancies, all payable to the institution; support to attend international scientific congresses), and grants, personal fees, and other from Celgene (support for costs of clinical trials, honoraria for speaker's fees and consultancies, all payable to the institution; support to attend international congresses), and Bristol-Myers Squibb (support for costs of clinical trials, honoraria for speaker's fees and consultancies, all payable to the institution; support to attend international scientific congresses) outside the submitted work and grants and other from Vertex (support for costs of clinical trials payable to the institution), Bayer (support for costs of clinical trials payable to the institution), AstraZeneca (support for costs of clinical trials payable to the institution), BeiGene (support for costs of clinical trials payable to the institution), and grants and other from Clovis (support for costs of clinical trials, honoraria for consultancies, all payable to the institution), Eisai (support for costs of clinical trials, honoraria for speaker's fees and consultancies, all payable to the institution), Genentech (support for costs of clinical trials, honoraria for consultancies, all payable to the institution), GlaxoSmithKline (support for costs of clinical trials, honoraria for speaker's fees and consultancies, all payable to the institution), Immunova (honoraria for consultancies, payable to the institution), Nucana (support for costs of clinical trials, honoraria for speaker's fees and consultancies, all payable to the institution), Karus Therapeutics (honoraria for consultancies, payable to the institution; member of scientific advisory board), Roche (support for costs of clinical trials, honoraria for speaker's fees and consultancies, all payable to the institution), MiNa Therapeutics (support for costs of clinical trials, payable to the institution), Pfizer (support for costs of clinical trials, payable to the institution), Sierra (support for costs of clinical trials, payable to the institution), Lilly (support for costs of clinical trials, payable to the institution), Novartis (support for costs of clinical trials, payable to the institution), Bicycle Therapeutics (support for costs of clinical trials, payable to the institution), Halozyme (support for costs of clinical trials, payable

to the institution), CytomX (support for costs of clinical trials, payable to the institution), Johnson & Johnson (support for costs of clinical trials, payable to the institution), Plexxikon (support for costs of clinical trials, payable to the institution), Boehringer (support for costs of clinical trials, payable to the institution), Athenex (support for costs of clinical trials, payable to the institution), Adaptimmune (support for costs of clinical trials, payable to the institution), Verastem (support for costs of clinical trials, payable to the institution), Iovance (support for costs of clinical trials, payable to the institution), Berg (support for costs of clinical trials, payable to the institution), BioLineRx (support for costs of clinical trials, payable to the institution), Basilea (support for costs of clinical trials, payable to the institution), grants and other from Medivir (support for costs of clinical trials, honoraria for speaker's fees and consultancies, all payable to the institution), and iOnctura (support for costs of clinical trials, payable to the institution) outside the submitted work. A. Anthoney reports grants from Immunocore (commercially funded clinical trial) during the conduct of the study, personal fees from ONO Pharmaceuticals UK, and grants from Novartis (grant to institute) outside the submitted work. A.N. Shoushtari reports grants and personal fees from Immunocore during the conduct of the study and Bristol-Myers Squibb, personal fees from Castle Biosciences, grants from Xcovery and Polaris outside the submitted work. O. Hamid reports personal fees from Array, BMS, Novartis, and Sanofi/Regeneron (speaker) and Aduro, Akeso, Amgen, Array, BeiGene, BMS, Genentech, GSK, Immunocore, Incyte, Janssen, Merck, NextCure, Novartis, Sanofi Regeneron, Seattle Genetics, Tempus, and Zelluna (consulting) during the conduct of the study, other from Arcus, Aduro, Akeso, Amgen, Array, BMS, CytomX, Exelixis, Genentech, GSK, Immunocore, Incyte, Iovance, Merck, Moderna, Merck Serono, NextCure, Novartis, Sanofi Regeneron, Seattle Genetics, Torque, and Zelluna (contracted research for institution) outside the submitted work. A. Gupta reports personal fees and non-financial support from Bristol Myers Squibb (consultancy fees and honoraria for educational meetings, non-financial support to attend conferences) and Novartis (consultancy fees and honoraria for educational meetings, non-financial support to attend conferences) and personal fees from Amgen (consultancy fees) outside the submitted work. E. Leach reports other from Syneos (article preparation) during the conduct of the study. R. Naidoo reports other from Syneos (article preparation) during the conduct of the study. S. Lewis reports employment with Immunocore Ltd. I. O'Kelly reports other from Immunocore (employment) outside the submitted work. M. Sznol reports personal fees from Immunocore (for consulting), Idera, Regeneron, Apexigen, Alligator, Verastem, Agenus, Rubius, BMS, Genentech-Roche, and Boston Pharma, Servier, Adaptimmune, Dragonfly, Pierre-Fabre, Molecular partners, Boehringer Ingelheim, Innate Pharma, Nektar, Pieris, Numab, AbbVie, Zelluna, Seattle Genetics, Genocea, GI Innovation, BioNTech, Lilly, Modulate, Array, AstraZeneca, Genmab, Novartis, and Incyte outside the submitted work, and other from Immunocore (funds to institution to cover costs of the trial) during the conduct of the study, Adaptive Biotech (stock options), Amphivena (stock options), Actym (stock options), Johnson and Johnson (stock), and GSK (stock), EvolveImmune (stock options and fees) and NextCure (stock options and fees) outside the submitted work. No potential conflicts of interest were disclosed by the other authors.

Disclaimer

The views expressed are those of the authors and not necessarily those of the NIHR or the Department of Health and Social Care.

Authors' Contributions

M.R. Middleton: Conceptualization, resources, writing-original draft, writing-review and editing. **C. McAlpine:** Formal analysis, writing-original draft, writing-review and editing. **V.K. Woodcock:** Investigation, writing-review and editing. **P. Corrie:** Investigation, writing-review and editing. **J.R. Infante:** Investigation. **N.M. Steven:** Investigation. **T.R.J. Evans:** Investigation. **A. Anthoney:** Investigation. **A.N. Shoushtari:** Investigation. **O. Hamid:** Investigation. **A. Gupta:** Investigation. **A. Vardeu:** Investigation. **E. Leach:** Formal analysis. **R. Naidoo:** Formal analysis. **S. Stanhope:** Formal analysis. **S. Lewis:** Formal analysis. **J. Hurst:** Formal analysis. **I. O'Kelly:** Writing-original draft, writing-review and editing. **M. Sznol:** Investigation, writing-review and editing.

Acknowledgments

The investigators are grateful to the patients, their care givers, and the study teams at participating sites for their support of this trial. The UK sites were supported by funding from Experimental Cancer Medicine Centre grants [Cancer Research UK, Department of Health (England) and Chief Scientist's Office (Scotland)]. M.R. Middleton was supported by the NIHR Oxford Biomedical Research Centre. We acknowledge everybody who contributed to the study including data acquisition, analysis, and interpretation in particular Bent Jakobsen, Koustubh Ranade, David Berman, Yvonne McGrath, David Krige, and Namir Hassan.

The costs of publication of this article were defrayed in part by the payment of page charges. This article must therefore be hereby marked *advertisement* in accordance with 18 U.S.C. Section 1734 solely to indicate this fact.

Received April 2, 2020; revised June 11, 2020; accepted August 14, 2020; published first August 18, 2020.

References

1. Wilson RAM, Evans TRJ, Fraser AR, Nibbs RJB. Immune checkpoint inhibitors: new strategies to checkmate cancer. Clin Exp Immunol 2018;191:133–48.
2. Ledford H. Cancer treatment: the killer within. Nature 2014;508:24–6.
3. Darvin P, Toor SM, Sasidharan Nair V, Elkord E. Immune checkpoint inhibitors: recent progress and potential biomarkers. Exp Mol Med 2018;50:165.
4. Lowe KL, Cole D, Kenefeck R, I OK, Lepore M, Jakobsen BK. Novel TCR-based biologics: mobilising T cells to warm 'cold' tumours. Cancer Treat Rev 2019;77:35–43.
5. Marshall HT, Djamgoz MBA. Immuno-oncology: emerging targets and combination therapies. Front Oncol 2018;8:315.
6. Rossjohn J, Gras S, Miles JJ, Turner SJ, Godfrey DI, McCluskey J. T cell antigen receptor recognition of antigen-presenting molecules. Annu Rev Immunol 2015;33:169–200.
7. de Souza JE, Galante PA, de Almeida RV, da Cunha JP, Ohara DT, Ohno-Machado L, et al. SurfaceomeDB: a cancer-orientated database for genes encoding cell surface proteins. Cancer Immun 2012;12:15.
8. Boudousquie C, Bossi G, Hurst JM, Rygiel KA, Jakobsen BK, Hassan NJ. Polyfunctional response by ImmTAC (IMCgp100) redirected CD8(+) and CD4(+) T cells. Immunology 2017;152:425–38.
9. Liddy N, Bossi G, Adams KJ, Lissina A, Mahon TM, Hassan NJ, et al. Monoclonal TCR-redirected tumor cell killing. Nat Med 2012;18:980–7.
10. Bossi G, Buisson S, Oates J, Jakobsen BK, Hassan NJ. ImmTAC-redirected tumour cell killing induces and potentiates antigen cross-presentation by dendritic cells. Cancer Immunol Immunother 2014;63:437–48.
11. Harper J, Adams KJ, Bossi G, Wright DE, Stacey AR, Bedke N, et al. An approved *in vitro* approach to preclinical safety and efficacy evaluation of engineered T cell receptor anti-CD3 bispecific (ImmTAC) molecules. PLoS One 2018;13:e0205491.
12. Armitage P, Berry G, Matthews J. Statistical methods in medical research. Hoboken, NJ: Wiley; 2002.
13. Gu Z, Eils R, Schlesner M. Complex heatmaps reveal patterns and correlations in multidimensional genomic data. Bioinformatics 2016;32:2847–9.
14. Lee DW, Gardner R, Porter DL, Louis CU, Ahmed N, Jensen M, et al. Current concepts in the diagnosis and management of cytokine release syndrome. Blood 2014;124:188–95.
15. Eisenhauer EA, Therasse P, Bogaerts J, Schwartz LH, Sargent D, Ford R, et al. New response evaluation criteria in solid tumours: revised RECIST guideline (version 1.1). Eur J Cancer 2009;45:228–47.
16. Groom JR, Luster AD. CXCR3 in T cell function. Exp Cell Res 2011;317:620–31.
17. Marshall E, Romaniuk C, Ghaneh P, Wong H, McKay M, Chopra M, et al. MRI in the detection of hepatic metastases from high-risk uveal melanoma: a prospective study in 188 patients. Br J Ophthalmol 2013;97:159–63.
18. Mulligan AM, Raitman I, Feeley L, Pinnaduwage D, Nguyen LT, O'Malley FP, et al. Tumoral lymphocytic infiltration and expression of the chemokine CXCL10 in breast cancers from the Ontario Familial Breast Cancer Registry. Clin Cancer Res 2013;19:336–46.
19. Yang X, Chu Y, Wang Y, Zhang R, Xiong S. Targeted *in vivo* expression of IFN-gamma-inducible protein 10 induces specific antitumor activity. J Leukoc Biol 2006;80:1434–44.
20. Bronger H, Singer J, Windmuller C, Reuning U, Zech D, Delbridge C, et al. CXCL9 and CXCL10 predict survival and are regulated by cyclooxygenase inhibition in advanced serous ovarian cancer. Br J Cancer 2016;115:553–63.

Published OnlineFirst August 18, 2020; DOI: 10.1158/1078-0432.CCR-20-1247

21. Kondo T, Ito F, Nakazawa H, Horita S, Osaka Y, Toma H. High expression of chemokine gene as a favorable prognostic factor in renal cell carcinoma. J Urol 2004;171:2171–5.
22. Mullins IM, Slingluff CL, Lee JK, Garbee CF, Shu J, Anderson SG, et al. CXC chemokine receptor 3 expression by activated CD8+ T cells is associated with survival in melanoma patients with stage III disease. Cancer Res 2004;64: 7697–701.
23. Suyama T, Furuya M, Nishiyama M, Kasuya Y, Kimura S, Ichikawa T, et al. Up-regulation of the interferon gamma (IFN-gamma)-inducible chemokines IFN-inducible T-cell alpha chemoattractant and monokine induced by IFN-gamma and of their receptor CXC receptor 3 in human renal cell carcinoma. Cancer 2005;103:258–67.
24. Li J, Ybarra R, Mak J, Herault A, De Almeida P, Arrazate A, et al. IFNgamma-induced chemokines are required for CXCR3-mediated T-cell recruitment and antitumor efficacy of anti-HER2/CD3 bispecific antibody. Clin Cancer Res 2018; 24:6447–58.
25. Chow MT, Ozga AJ, Servis RL, Frederick DT, Lo JA, Fisher DE, et al. Intratumoral activity of the CXCR3 chemokine system is required for the efficacy of anti-PD-1 therapy. Immunity 2019;50:1498–512.
26. Damato BE, Dukes J, Goodall H, Carvajal RD. Tebentafusp: T cell redirection for the treatment of metastatic uveal melanoma. Cancers 2019;11:971.
27. Damato B. Progress in the management of patients with uveal melanoma. The 2012 Ashton lecture. Eye 2012;26:1157–72.
28. Krantz BA, Dave N, Komatsubara KM, Marr BP, Carvajal RD. Uveal melanoma: epidemiology, etiology, and treatment of primary disease. Clin Ophthalmol 2017;11:279–89.
29. Lorenzo D, Piulats JM, Ochoa M, Arias L, Gutierrez C, Catala J, et al. Clinical predictors of survival in metastatic uveal melanoma. Jpn J Ophthalmol 2019;63: 197–209.
30. Khoja L, Atenafu EG, Suciu S, Leyvraz S, Sato T, Marshall E, et al. Meta-analysis in metastatic uveal melanoma to determine progression-free and overall survival benchmarks: an international rare cancers initiative (IRCI) ocular melanoma study. Ann Oncol 2019;30:1370–80.
31. Carvajal RD, Schwartz GK, Tezel T, Marr B, Francis JH, Nathan PD. Metastatic disease from uveal melanoma: treatment options and future prospects. Br J Ophthalmol 2017;101:38–44.
32. Yarchoan M, Hopkins A, Jaffee EM. Tumor mutational burden and response rate to PD-1 inhibition. N Engl J Med 2017;377:2500–1.

AACR American Association for Cancer Research

Clinical Cancer Research

Tebentafusp, A TCR/Anti-CD3 Bispecific Fusion Protein Targeting gp100, Potently Activated Antitumor Immune Responses in Patients with Metastatic Melanoma

Mark R. Middleton, Cheryl McAlpine, Victoria K. Woodcock, et al.

Clin Cancer Res Published OnlineFirst August 18, 2020.